

## Crystal chemistry of Fe<sup>3+</sup>, H<sup>+</sup>, and D/H in mantle-derived augite from Dish Hill: Implications for alteration during transport

M. DARBY DYAR,<sup>1</sup> SUZETTE V. MARTIN,<sup>2</sup> STEPHEN J. MACKWELL,<sup>3</sup> SUSAN CARPENTER,<sup>3</sup>  
CHRISTOPHER A. GRANT<sup>4</sup> and ANNE V. MCGUIRE<sup>5</sup>

<sup>1</sup>Department of Geology and Astronomy, West Chester University, West Chester, PA 19383, U.S.A.

<sup>2</sup>Mathematics and Science Department, Navajo Community College, P.O. Box 580, Shiprock, Navajo Nation, NM 87420, U.S.A.

<sup>3</sup>Department of Geosciences, The Pennsylvania State University, University Park, PA 16802, U.S.A.

<sup>4</sup>Department of Chemistry, University of Oregon, Eugene, OR 97403, U.S.A.

<sup>5</sup>Department of Geosciences, University of Houston, Houston, TX 77204, U.S.A.

**Abstract**—Chemical and crystal chemical analyses have been performed on a suite of sub-continental, mantle-derived augite samples and their accompanying magmas from a single cinder cone at Dish Hill, California. Mössbauer techniques have been used to investigate Fe oxidation state, uranium-extraction techniques have been used to determine bulk wt%H<sub>2</sub>O contents and D/H ratios, wet chemistry has been used to corroborate Fe<sup>3+</sup>/ΣFe, and electron microprobe techniques coupled with the above measurements have been used to determine major element contents of pyroxene. Comparison of Mössbauer and wet chemical results on Fe<sup>3+</sup>/Fe<sup>2+</sup> permitted determination of empirical correction factors that can be used to bring Mössbauer results of various fitting models into agreement with true Fe<sup>3+</sup>/Fe<sup>2+</sup> ratios, which range from 0.16 to 1.53. D/H ratios of augite samples range from -93.0‰ to -154.3‰, possibly suggesting exchange with meteoric waters, while the entraining basalts have somewhat heavier D/H ratios in the range -87.0‰ to -102.2‰, also indicating the likelihood of some exchange with surface waters. Results of experimental work to determine hydrogen diffusivity in high-Fe clinopyroxene, when applied to the Dish Hill augite, suggest that the augite megacrysts have exchanged hydrogen with the basaltic melts during ascent. However, as the time scale for transport is short, it is possible that equilibration of deuterium in the augite with that of the surrounding basalts may not have occurred. Differences in D/H ratios in the augite probably result from hydrogen exchange with the basalt during transport, and therefore do not reflect conditions in the mantle source region. The lack of a correlation between hydrogen remaining in the augite samples and Fe<sup>3+</sup>/Fe<sup>2+</sup> may therefore either result from the large uncertainties in the bulk hydrogen analysis or reflect significant variability in H<sup>+</sup> or Fe<sup>3+</sup> in the source region.

### INTRODUCTION

PIONEERING STUDIES by Roger Burns and Michael Bancroft on the electrochemical states of iron in pyroxene minerals were among the first investigations using the techniques of optical and Mössbauer spectroscopy in the study of minerals (BURNS, 1966; BANCROFT and BURNS, 1967; BANCROFT *et al.*, 1967a). These early studies are still cited frequently, particularly in the context of studies on Fe in pyroxenes with high pressure and temperature (upper mantle) compositions. Although his later interests expanded to include a wide variety of theoretical and experimental problems dealing with transition metal-bearing minerals, Roger Burns' interest in common rock-forming minerals and his respect for the geologic problems they could solve remained strong throughout his long career. He was never too busy to explain crystal chemistry to his geologic colleagues who came bearing questions. It seems appropriate, therefore, to dedicate this study of augite from the upper mantle to the broad-thinking genius and memory of Roger Burns.

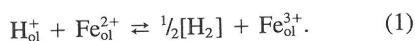
Until very recently, research programs assessing

the water contents, intrinsic oxygen fugacity, and hydrogen transport in the minerals of the Earth's upper mantle have proceeded largely independently, with minimal interaction between groups. For example, studies by Rossman and coworkers (MILLER *et al.*, 1987; SKOGBY and ROSSMAN, 1989, SKOGBY *et al.*, 1990 and 1992; SMYTH and ROSSMAN, 1991; BELL and ROSSMAN, 1992) pioneered standards and techniques for quantitative measurement of water contents in mantle phases, with emphasis on olivine, pyroxene, garnet and amphibole. Their work has shown that incorporation of small amounts of structurally-bound hydroxyl is ubiquitous in nominally anhydrous minerals from mantle xenoliths. Their conclusions have profound implications for the accommodation of water in the upper mantle. However, their studies were focussed primarily on characterization of hydroxyl contents, and have largely neglected experimental determination of the mechanisms by which hydroxyl contents of mantle phases may have been altered during transport.

Studies of mantle  $f_{O_2}$  have also utilized measure-

ments of as-erupted  $\text{Fe}^{3+}/\text{Fe}^{2+}$  contents in xenoliths to infer mantle conditions. Research by this group (DYAR *et al.*, 1989 and 1992; MCGUIRE *et al.*, 1989 and 1991), Wood and coworkers (WOOD and VIRGO, 1989; BRYNDZIA and WOOD, 1989; LUTH *et al.*, 1990; LUTH and CANIL, 1993), and others has characterized the  $\text{Fe}^{3+}/\text{Fe}^{2+}$  contents of olivine, pyroxene, spinel, garnet, and amphibole. This body of research has been widely used to derive estimates of upper mantle  $f_{\text{O}_2}$ , again with little consideration of the effects of hydrogen diffusion during transport on the  $\text{Fe}^{3+}/\text{Fe}^{2+}$  contents of as-erupted samples.

Meanwhile, a largely separate body of work within the geophysics community addresses the kinetics of hydrogen diffusion. MACKWELL and KOHLSTEDT (1990) showed that hydrogen diffusion in olivine is extremely rapid, facilitating the loss of  $\text{H}^+$  via the mechanism



Further work by BAI and KOHLSTEDT (1992) suggested that  $\text{H}^+$  contents of as-erupted olivine may therefore be under-representative of actual mantle conditions. Although these studies postulated a correlation between  $\text{H}^+$  and  $\text{Fe}^{3+}$  via the dehydrogenation reaction (eqn. 1 above),  $\text{Fe}^{3+}$  contents were not actually measured. This was also true of a recent study of hydrogen diffusion in a diopside single crystal (INGRIN *et al.*, 1995), where diffusivities fast enough to account for significant modification of  $\text{Fe}^{3+}$  (not measured) and  $\text{H}^+$  (measured) contents were observed. However, in an earlier study on synthetic magnesian clinopyroxene, SKOGBY (1994) did observe a near 1:1 correlation between  $\text{H}^+$  incorporated in clinopyroxene and  $\text{Fe}^{2+}$  increase. For amphibole, measured  $\text{Fe}^{3+}$  and  $\text{H}^+$  data were reported by DYAR *et al.* (1993), who used results from GRAHAM *et al.* (1984) to demonstrate that dehydrogenation of hornblende occurs more slowly than in olivine or pyroxene, leading to only minor modification of mantle  $\text{H}^+$  and  $\text{Fe}^{3+}$  during transport. This suggests that as-erupted  $\text{H}^+$  and  $\text{Fe}^{3+}$  contents of amphibole may directly reflect mantle equilibrium conditions, a conclusion that was also reached by BELL and HOERING (1994). Data on  $\text{H}^+$  diffusion in orthopyroxene, spinel, and garnet are currently being investigated (S. MACKWELL, personal communication; H. SKOGBY, personal communication). In summary, as-erupted  $\text{Fe}^{3+}$  and  $\text{H}^+$  contents of olivine and clinopyroxene may be substantially modified during transport, while amphibole is much less affected by ascent.

Accordingly, in the present study we seek to measure and understand the interrelationships be-

tween  $\text{H}_2\text{O}$  and  $\text{Fe}^{3+}$  in augite and Fe-rich diopside. We apply new data on hydrogen diffusivity in Fe-rich diopside compositions to our results on  $\text{Fe}^{3+}$ ,  $\text{H}^+$ , and D/H ratios in a suite of mantle-derived augite samples collected from a single cinder cone at Dish Hill, California. Hydrogen isotope data on augite are then compared with results on the host magmas at this locality, and with previous work on Dish Hill amphibole megacrysts (DYAR *et al.*, 1993; BELL and HOERING, 1994). Through this detailed study of naturally-occurring augite samples and applicable experimental results on Fe-rich diopside, we can assess 1) the isotopic and crystal chemical variation among samples from a single cinder cone, 2) the relationship(s) among  $\text{H}^+$ ,  $\text{Fe}^{3+}$ , and other major elements within the augite structure, and 3) the extent to which the compositions of the natural samples are in any way representative of mantle equilibria.

## BACKGROUND

### *Geology of Dish Hill*

The Dish Hill locality was chosen for this study for three important reasons. First, in order to rule out the effects of tectonic setting, this locality was chosen to provide an example of a single eruptive event. Second, the cone is extremely rich in megacrysts (as well as xenoliths), facilitating sampling of a number of large augite single crystals. The area was also the site of hornblende studies by BELL and HOERING (1994). Finally, the chemistry of the magmas that coexist with the augite megacrysts has been relatively well studied in the context of the southern California basaltic volcanoes (WILSHIRE *et al.*, 1986 and 1988).

Dish Hill is a cinder cone of basanite. Fission-track age dating shows the cone to be approximately 2 Ma old (WILSHIRE and TRASK, 1971). The present study used samples of the Dish Hill basanite and single crystals of augite (megacrysts), ranging from 1 cm to several cms in diameter (Table 1), found as inclusions within the host basalt. The megacrysts possess rounded glassy margins implying disequilibrium with the host basalt at the time of eruption. These megacrysts are likely to be either xenocrysts, fragments of augite from aluminous-augite pyroxene mantle rocks, or phenocrysts crystallized from the host magmas at mantle pressures. Aluminous augite pyroxenite xenoliths commonly form dikes or veins in mantle peridotite, which are generally inferred to originate by crystallization of mafic alkalic magmas within the mantle (*e.g.*, FREY and PRINZ, 1978). Whether they are xenocrysts or phenocrysts, the megacrysts in this

Table 1. Physical Characteristics of Augite Samples.\*

Sample Number	Weight in g** as collected	Maximum Dimensions of Megacryst, in cm		
DH-201	7.10	2.70	0.95	1.20
DH-202	47.39	3.70	2.10	3.40
DH-203	10.45	2.70	0.80	1.90
DH-204	9.35	3.40	1.20	2.20
DH-205	19.35	3.90	1.20	2.00
DH-206	18.70	2.50	1.50	2.40
DH-207	5.45	2.20	1.00	1.90
DH-209	38.90	3.40	2.20	2.80
DH-210	40.40	3.30	2.30	2.50
DH-211	204.10	2.40	0.60	1.40
DH-212	20.95	2.30	1.50	0.40
DH-213	299.80	3.10	1.80	1.20
DH-217	n.d.	1.30	1.10	n.d.
DH-218	n.d.	3.00	1.80	n.d.
DH-220	n.d.	2.20	1.84	n.d.
DH-222	n.d.	1.55	1.10	n.d.
DH-227	n.d.	1.60	1.12	n.d.
DH-231	n.d.	1.90	1.10	n.d.

\*All samples showed evidence of slight melting on some edges.

\*\*Includes sample and its attached lava matrix.

n.d. = Some samples were crushed before complete measurements were obtained.

study are presumed to be the products of crystallization of alkalic basalts at mantle pressures, and thus their measured  $\text{Fe}^{3+}/\text{Fe}^{2+}$  and D/H ratios should provide information about  $f_{\text{O}_2}$  and D/H of the mafic magma within the mantle, unless these ratios are altered during transport and eruption of the host magma.

#### $\text{H}^+$ Contents of Pyroxene

This subject is well reviewed in the work by Rossman and coworkers (see, especially, SKOGBY *et al.*, 1990; SMYTH *et al.*, 1991, and BELL, 1993). Only two aspects of these studies bear upon the present work. First, the existing IR studies show that mantle derived diopside, omphacite, and augite are all significant reservoirs for  $\text{OH}^-$ . Reported hydrogen contents for as-erupted clinopyroxene samples range up to 620 ppm  $\text{H}_2\text{O}$  (BELL, 1993), and suggest that clinopyroxene has the highest  $\text{OH}^-$  contents of the volumetrically significant "anhydrous" minerals in the mantle. Second, the determination of clinopyroxene  $\text{OH}^-$  contents is precise and relatively straightforward by the FTIR technique, BUT accurate quantitative measurements have been hampered by the lack of mineral-specific

calibration standards for  $\text{OH}^-$ . Even when such well-characterized standards are used, determination of  $\text{OH}^-$  contents in upper mantle pyroxenes may have uncertainties ranging from  $\pm 10\%$  to  $\pm 50\%$  depending on composition (BELL, 1993). For this reason, and because of our interest in D/H as well as  $\text{H}_2\text{O}$  contents of our samples, we have chosen in this study to use manometric methods for hydrogen extraction from augite instead of FTIR. Although the extraction technique brings its own inherent errors to our work (see Methods section below), it does avoid the calibration problems associated with FTIR.

#### $\text{Fe}^{3+}$ Contents of Pyroxene

The technique of Mössbauer spectroscopy has been used in numerous studies of the  $\text{Fe}^{3+}$  contents of mantle clinopyroxene, as reviewed in DYAR *et al.* (1989). More recently, the methodology of the Mössbauer experiment has been examined in detail and refinements have been made that improve its accuracy. LUTH and CANIL (1993) tested the effects of absorber thickness on a single clinopyroxene sample from British Columbia and found constant values within experimental error of  $\text{Fe}^{3+}/\Sigma\text{Fe}$  over a concentration range of 2–5 mg  $\text{Fe}/\text{cm}^2$ . Because our samples have nearly identical bulk compositions to the sample studied by LUTH and CANIL (1993), we might assume that for samples prepared within that concentration range, and having similar  $\text{Fe}^{3+}$  and total Fe contents, absorber thickness should have little effect on the measured  $\text{Fe}^{3+}/\Sigma\text{Fe}$  values. However, this presumes that the relative amounts and distributions of all species on sites are also similar.

A more significant problem in the determination of  $\text{Fe}^{3+}/\Sigma\text{Fe}$  values by Mössbauer spectroscopy is the differential recoil-free fractions ( $f$ ) of Fe atoms having different oxidation states (WHIPPLE, 1972; AMTHAUER *et al.*, 1976; DEGRAVE and VAN ALBOOM, 1991; DYAR *et al.*, 1993). This effect arises because  $\text{Fe}^{3+}$  atoms are more tightly bound into their sites than are less highly charged  $\text{Fe}^{2+}$  atoms, resulting in  $f_{\text{Fe}^{3+}}$  being generally higher than  $f_{\text{Fe}^{2+}}$ . Differences have also been observed in the recoil-free fractions of Fe atoms having the same oxidation state but located in different crystallographic sites (BANCROFT *et al.*, 1967b; DEGRAVE and VAN ALBOOM, 1991).

The area of a Mössbauer doublet depends explicitly on the absorber recoil-free fraction (PRESTON *et al.*, 1962; BANCROFT, 1967; BANCROFT, 1969). In conventional analysis, ratios of peak areas are used to determine site population or redox ratios.

More completely, the areal ratio is proportional to the true redox ratio:

$$\frac{A_{Fe^{3+}}}{A_{Fe^{2+}}} = C \frac{N(Fe^{3+})}{N(Fe^{2+})}, \quad (2)$$

where

$$C = \frac{\Gamma_{Fe^{3+}} f_{Fe^{3+}} G(x)_{Fe^{3+}}}{\Gamma_{Fe^{2+}} f_{Fe^{2+}} G(x)_{Fe^{2+}}}, \quad (3)$$

and  $N$  is the amount of each species actually present,  $f$  is the site-specific recoil-free fraction,  $\Gamma$  is peak width, and  $G(x)$  is a saturation term (a similar expression may be constructed for site-population ratios). Commonly, it is assumed that  $\Gamma_{Fe^{2+}} = \Gamma_{Fe^{3+}}$ ,  $f_{Fe^{2+}} = f_{Fe^{3+}}$ , and  $G(x)_{Fe^{2+}} = G(x)_{Fe^{3+}}$ , so that  $C = 1.0$ . In general,  $f_{Fe^{2+}} \neq f_{Fe^{3+}}$  (WHIPPLE, 1972; DEGRAVE and VAN ALBOOM, 1991; KARFUNKEL and POLLAK, 1993).

To the extent that  $f$  values are known (and caution must be used here, because  $f$  is sensitive to mineral composition) in principle it is possible to calculate "true"  $Fe^{3+}/\Sigma Fe$  values for given minerals by determining an appropriate value for  $C$ . However, complications arise when a mineral contains Fe in more than one type of crystallographic site AND more than one oxidation state. In the case of clinopyroxene, both  $Fe^{3+}$  and  $Fe^{2+}$  are present, and may be distributed between the M2 and M1 sites (and/or in the tetrahedral site if the composition is Si- and Al-deficient, but such samples will not be considered here). Ideally this distribution of species should be treated as:

$$\frac{A_{Fe^{3+}}^{M1}}{A_{Fe^{2+}}^{M1} + A_{Fe^{2+}}^{M2}} = \frac{f_{Fe^{3+}}^{M1} N(Fe^{3+})^{M1}}{f_{Fe^{2+}}^{M1} N(Fe^{2+})^{M1} + f_{Fe^{2+}}^{M2} N(Fe^{2+})^{M2}}. \quad (4)$$

For diopside,  $f_{Fe^{3+}}^{M1}$  and  $f_{Fe^{2+}}^{M1}$  have been experimentally determined to be 0.862 and 0.708, respectively, at room temperature (DEGRAVE and VAN ALBOOM, 1991), but there has been no comparable determination of  $f_{Fe^{2+}}^{M2}$ . Also, SKOGBY *et al.* (1992) demonstrated that for orthopyroxene,  $f_{Fe^{2+}}^{M2}$  and  $f_{Fe^{2+}}^{M1}$  are different. In our samples, the site-specific recoil-free fractions are all different, and there is no way to formulate a simple constant,  $C$ , that depends on recoil-free fractions and that can be used to extract "true" redox ratios from Mössbauer peak-area ratios.

A final complication in the derivation of "true"  $Fe^{3+}/\Sigma Fe$  values from Mössbauer peak areas arises from the use of different models for interpreting the Mössbauer data. Historically, mineralogical studies

have employed Lorentzian line shapes, using the assumptions inherent in the thin absorber approximation. Although it has been generally recognized that other line shapes such as Voigt lines (LANG, 1963; EVANS and BLACK, 1970) may be more appropriate, use of these improved line shapes has until recently been computationally intractable, particularly when processing large numbers of different samples. In this study we have calculated  $Fe^{3+}/Fe^{2+}$  values for spectra fit with a number of different models including eight and six Lorentzian lines and four Voigt lines. Using this strategy, we have derived appropriate correction terms that bring the results of the various fitting models into agreement with true  $Fe^{3+}/Fe^{2+}$  ratios as determined by wet chemistry.

#### SAMPLE SELECTION, PREPARATION, AND ANALYSES

Augite megacrysts were collected for this study by M.D.D. and A.V.M., with the assistance of co-participants in a U.S.G.S.-sponsored workshop on mantle composition, structure, and processes. Samples were collected from the south flank of the Dish Hill cinder cone adjacent to the north side of the railroad bridge. Specimens were weighed and measured before removing small pieces for thin sections. Additional pieces were broken off and ground by hand with constant wetting using acetone (to prevent oxidation) into fragments <1 mm to facilitate hand-picking of grains. Only pristine augite grains were used for this study; any grains containing visible alteration, inclusions, or impurities were rejected. In particular, we sought to use only the interior portions of megacrysts to guard against contamination by surface carbonate and to avoid the need to wash the samples in acid and risk modification of D/H. Approximately 530 mg of separates were prepared from each sample: 150 mg for Mössbauer analyses, 50 mg for wet chemistry, 300 mg for  $H^+$  extraction, and 30 mg for future oxygen isotope study. Basalt samples were collected for us by Howard Wilshire; clean splits were crushed and prepared for isotopic analysis by the U.S. Geological Survey.

Electron microprobe analyses were performed at the University of Houston using the JEOL 8600 Superprobe with Noran (Tracor Northern) automation. Natural and synthetic mineral standards were used and matrix correction was done by the Noran ZAF routine. Routine analytical conditions were used: 15 keV acceleration voltage, 20 nA beam current measured on a Faraday cup, 40 s count times (20 s count time on sodium), and a 10  $\mu m$  beam diameter. At least 5 points were analyzed on each megacryst. Probe scans were used to screen for zoning, and to eliminate zoned samples from this study. Analytical errors are  $\pm 0.5$ –2% for major elements and  $\pm 10$ –20% for minor elements.

Mössbauer analyses were performed in the Mineral Spectroscopy Laboratory at West Chester University. A source of 50–20 mCi  $^{57}Co$  in Pd was used on an Austin Science Associates constant acceleration spectrometer. Results were calibrated against an  $\alpha$ -Fe foil of 6  $\mu m$  thickness and 99.99% purity. Spectra were folded at a channel number selected by use of autocorrelation to en-

sure the proper match of peak positions after folding. Spectra were fitted using a version of the program STONE modified to run on IBM and compatible personal computers. The program uses a nonlinear regression procedure with a facility for constraining any set of parameters or linear combination of parameters. Lorentzian and Voigt line shapes were used for resolving peaks as discussed above. Fitting procedures in general followed those described by DYAR *et al.* (1989) and MCGUIRE *et al.* (1989), with modifications described by GRANT (1995). A statistical best fit was obtained using each model for each spectrum using the  $\chi^2$  and/or Misfit parameters; practical application of these parameters is discussed elsewhere (DYAR, 1984; GRANT, 1995). Errors are estimated at  $\pm 1\%$  for doublet areas, and  $\pm 0.02$  mm/s for peak width, isomer shift, and quadrupole splitting.

Hydrogen contents were determined by means of a procedure for collecting and measuring all the structural hydrogen using a volumetric measurement of water vapor extracted from silicates (see BIGEISEN *et al.*, 1952 and HOLDAWAY *et al.*, 1986 for details of the technique). For this study, 300 mg of each sample were weighed into molybdenum crucibles, then degassed under vacuum for at least 8 h at 50–85°C to drive off adsorbed atmospheric moisture. Samples were then fused in an induction furnace to liberate structural water. Distillation processes involving transfer of evolved gases through a series of liquid nitrogen and methanol-dry ice slush traps were used to separate water molecules effectively from other condensible and non-condensable gases. Water vapor was then passed over a hot ( $>750$  °C) uranium furnace to liberate free  $H^+$ . A mercury-piston Toepler pump was used to collect hydrogen vapor in a volumetrically calibrated reservoir for yield measurement. Approximately half the samples were run at least twice. Distilled  $H_2O$  was used for calibration. All data are corrected for the blank of 2.5 torr that arises from degassing of the crucibles. Errors are estimated at  $\leq 0.1$  wt%  $H_2O$  based on replications.

Wet chemical determinations of  $Fe^{3+}/\Sigma Fe$  were determined by analyst Jun Wu in the laboratory of Joseph Stucki at the University of Illinois, using methods developed by Stucki for clay minerals. His colorimetric method (STUCKI, 1981; STUCKI and ANDERSON, 1981; KOMANDEL and STUCKI, 1988) includes an organic chromophore during the sample digestion which complexes the iron as it is released into solution, thereby protecting against aerial oxidation. This method has a greater specificity for iron than do oxidimetric methods. In the analyses, 1,10-phenanthroline (phen) is used, which forms a red complex with  $Fe^{2+}$  and a colorless complex with  $Fe^{3+}$ . Several aspects of this procedure are significant. First, Stucki's group has done an extensive analysis of the sources of variability in the method. Second, they have demonstrated that the instability of the  $Fe^{3+}$ -phen complex, which bedeviled earlier colorimetric analyses using phen, is due to photoreduction and can be eliminated by excluding light. Third, the photoreduction of the  $Fe^{3+}$ -phen complex to the  $Fe^{2+}$ -phen complex can be carried out quantitatively. Samples are digested while excluding light,  $Fe^{2+}$  is measured colorimetrically, the sample is exposed to light to reduce all  $Fe^{3+}$ , and finally  $Fe^{2+}$  is measured again, this time to obtain total iron. Thus, both  $Fe^{2+}$  and total iron are obtained from a single dissolution. Errors based on 10 replicate analyses of geochemical reference standards are  $\pm 0.01$ – $0.03\%$  of the % of Fe species (*e.g.*,  $Fe^{2+}$  or  $Fe^{3+}$ ) present (J. STUCKI, personal communication, 1995). Errors on the wet chemical analyses of our samples

are at least as good as  $\pm 0.1\%$  of the % $Fe^{2+}$  present, or approximately  $\pm 0.07$  of the %Fe for each species.

Single crystal diopside samples ( $Ca_{0.965}Mg_{0.946}Fe_{0.065}Si_2O_6$ ) from Jaipur in India (CARPENTER, 1996) were used for the hydrogen diffusivity experiments, which are somewhat more iron-rich than those in the study reported by INGRIN *et al.* (1995). The experiments were performed in a 1-bar controlled-atmosphere furnace at 750° and 810°C, with the oxygen fugacity controlled by using CO/CO<sub>2</sub> gases at  $10^{-10-14.0 \pm 0.5}$  atm (near the Ni/NiO buffer), for time lengths from 1 to 100 hours. The hydrogen contents were measured from unpolarized infrared spectra obtained using a Fourier transform infrared spectrometer in the wavelength range from 4000 to 2000  $cm^{-1}$ . Using the integral absorbance for a series of bands near 3500  $cm^{-1}$ , resulting from O-H stretching vibrations, and an integral molar absorption coefficient of 1.0  $cm^{-2}$  per  $H/10^{16}Si$  (PATERSON, 1982), we were able to calculate water contents as a function of the length of time of heat treatment. Although the extinction coefficients have not been determined explicitly for O-H absorption bands in diopside, we have assumed a value typical of O-H bands in other silicates (PATERSON, 1982); we note that our diffusion analysis is insensitive to the absolute values of water content and only depends on the relative results from a sequence of measurements on an individual sample.

## RESULTS

### *Chemical formulae*

Chemical compositions for all samples and for the average of all samples from Dish Hill determined by electron probe, corrected Mössbauer, and H-extraction techniques as described above are given in Table 2. The FeO and  $Fe_2O_3$  contents were calculated from the electron probe data using Mössbauer results corrected to "true"  $Fe^{3+}/Fe^{2+}$  using the empirical correction factors discussed below. Data were normalized to formula units with 6 oxygens, and iterated to ensure charge balance.

Cation data from the analyses show that  $\Sigma(Ca+Na+K)$  is always considerably less than one formula unit, requiring the substitution of some combination of divalent cations to fill the site. In most cases, even the addition of the all the  $Fe^{2+}$  determined for the sample cannot completely fill the M2 site; thus it is apparent that some Mg must occupy M2. The tetrahedral sites are systematically low in Si, requiring the substitution of Al or  $Fe^{3+}$  to fill them. These compositional characteristics place constraints on the interpretation of the site occupancy data provided by the Mössbauer work, because the presence of tetrahedral  $Fe^{3+}$  will change the shape of the spectral absorption profile. However, without corroborating X-ray structure refinement data, it is unclear whether Al or  $Fe^{3+}$  fills the tetrahedral sites. It is also possible that sufficient concentrations of vacant lattice sites may be present to affect stoichiometry in the minerals, although we have no evidence to support or refute this possibility.

Table 2. Augite Compositions

	DH-201	DH-202	DH-203	DH-204	DH-205	DH-206	DH-207	DH-209	DH-210	DH-211	DH-212	DH-213	DH-217	DH-218	DH-220	DH-222	DH-227	DH-231
SiO <sub>2</sub>	48.25	47.87	48.07	47.45	47.74	47.29	45.91	50.89	50.08	47.71	47.22	47.74	47.17	47.34	47.97	47.55	47.56	47.52
Al <sub>2</sub> O <sub>3</sub>	9.11	9.44	9.27	9.15	9.42	9.35	8.86	6.64	7.80	9.01	9.39	9.41	9.26	9.30	9.25	9.33	9.31	9.15
TiO <sub>2</sub>	1.42	1.53	1.35	1.79	1.54	1.85	2.04	0.70	0.67	1.50	2.25	1.63	1.78	1.72	1.34	1.61	1.78	1.70
FeO	4.73	4.92	4.96	5.33	5.09	5.30	7.50	3.98	3.79	5.00	5.39	4.64	5.18	5.08	5.19	5.32	5.31	5.31
Fe <sub>2</sub> O <sub>3</sub>	2.33	2.27	2.21	2.76	2.53	2.78	4.26	1.66	1.87	2.87	2.52	2.80	2.72	2.96	2.51	2.62	2.92	3.09
MgO	14.23	14.17	14.27	13.36	14.12	13.28	9.49	17.11	16.51	13.94	13.83	13.77	13.39	13.56	14.23	13.61	13.22	13.35
MnO	0.15	0.15	0.16	0.15	0.16	0.15	0.34	0.15	0.13	0.18	0.15	0.16	0.15	0.16	0.16	0.16	0.15	0.16
Cr <sub>2</sub> O <sub>3</sub>	0.00	0.01	0.01	0.00	0.00	0.00	0.00	0.57	0.45	0.00	0.12	0.01	0.00	0.01	0.01	0.00	0.00	0.01
CaO	19.54	19.60	19.64	19.54	19.13	19.74	20.96	18.44	18.46	19.30	18.48	19.48	19.76	19.26	18.92	19.55	19.45	19.39
Na <sub>2</sub> O	1.11	1.09	1.04	1.25	1.17	1.20	1.79	0.95	1.03	1.21	1.32	1.18	1.23	1.24	1.19	1.16	1.30	1.24
F	0.07	0.04	0.50	0.01	0.00	0.02	0.03	0.03	0.02	0.08	0.04	0.03	0.01	0.00	0.02	0.07	0.03	0.03
H <sub>2</sub> O	0.18	0.07	0.86	0.06	0.06	0.06	0.13	0.16	0.07	0.05	0.13	0.09	0.07	0.11	0.12	0.05	0.07	0.10
Total	101.11	101.16	102.33	100.85	100.95	101.02	101.30	101.29	100.88	100.85	100.84	100.94	100.72	100.74	100.91	101.03	101.10	101.05
Fe <sup>3+</sup> /ΣFe	30.7	29.3	28.6	31.8	30.9	32.1	33.8	27.3	30.7	34.1	29.6	35.2	32.1	34.4	30.3	30.7	33.1	34.4
Si	1.731	1.730	1.578	1.736	1.740	1.725	1.706	1.816	1.799	1.722	1.714	1.731	1.728	1.733	1.742	1.718	1.730	1.729
Al	0.385	0.402	0.359	0.395	0.405	0.402	0.388	0.279	0.330	0.383	0.402	0.402	0.400	0.401	0.396	0.397	0.399	0.392
Ti	0.038	0.042	0.033	0.049	0.042	0.051	0.057	0.019	0.018	0.041	0.061	0.044	0.049	0.047	0.037	0.044	0.049	0.047
Fe <sup>3+</sup>	0.142	0.149	0.136	0.163	0.155	0.162	0.233	0.119	0.114	0.151	0.164	0.141	0.159	0.155	0.158	0.161	0.162	0.162
Fe <sup>2+</sup>	0.063	0.062	0.055	0.076	0.069	0.076	0.119	0.045	0.050	0.078	0.069	0.076	0.075	0.082	0.069	0.071	0.080	0.085
Mg	0.761	0.763	0.698	0.729	0.767	0.722	0.526	0.910	0.884	0.750	0.748	0.744	0.731	0.740	0.770	0.733	0.717	0.724
Mn	0.005	0.005	0.004	0.005	0.005	0.005	0.011	0.005	0.004	0.006	0.005	0.005	0.005	0.005	0.005	0.005	0.005	0.005
Cr	0.000	0.000	0.000	0.000	0.000	0.000	0.000	0.016	0.013	0.000	0.003	0.000	0.000	0.000	0.000	0.000	0.000	0.000
Ca	0.751	0.759	0.691	0.766	0.747	0.772	0.834	0.705	0.710	0.747	0.719	0.757	0.776	0.756	0.736	0.757	0.758	0.756
Na	0.077	0.076	0.066	0.089	0.083	0.085	0.129	0.066	0.072	0.085	0.093	0.083	0.087	0.088	0.084	0.081	0.092	0.087
F	0.008	0.005	0.052	0.001	0.000	0.002	0.004	0.003	0.002	0.009	0.005	0.003	0.001	0.000	0.002	0.008	0.003	0.003
H	0.042	0.017	0.188	0.015	0.015	0.015	0.031	0.038	0.017	0.012	0.031	0.022	0.017	0.027	0.029	0.012	0.017	0.024

*H<sup>+</sup> contents*

Hydrogen data collected in this study show a range of water contents from 0.05–0.21 wt% H<sub>2</sub>O for 17 of the 18 samples. These values are consistent with the ranges observed in previous studies. The interesting outlier is sample DH-203, which has a very unusual H<sub>2</sub>O content of 0.86 wt%. IR study of this sample is underway to confirm this unusually high value. It is tempting to discard this analysis except for the fact that this sample is also distinct by virtue of low Ca, Si, and Mg accompanied by high F and H. Perhaps this sample originated in a different compositional regime of the upper mantle from the other samples in the suite. Alternatively, it may have reacted with a metasomatic fluid with unusually high F and H contents.

Hydrogen isotope values for the augite samples range from –93.0‰ up to –154.3‰, strongly suggesting contact and exchange with meteoric waters either during ascent or cooling (Table 3). The entraining basalts have heavier D/H ratios, falling in

a narrower range between –87.0‰ and –102.2‰. It must be noted that contamination from meteoric waters (locally about –46 to –99‰, according to data from INTERNATIONAL ATOMIC ENERGY AGENCY, 1979) is not the only plausible explanation for the observed deuterium depletions. Such compositions are known from mantle sources, having been measured in mantle-derived amphiboles and interpreted using similar arguments to those presented here (DELOULE *et al.*, 1991). However, both basalts and augite samples are distinctly different from hornblende megacrysts previously reported from the Dish Hill locality, which have D/H ratios of  $-46.8 \pm 7.7\%$  (BELL and HOERING, 1994) that can be interpreted as mantle values. Therefore, the difference between the D/H of the augites and basalts vs. the Dish Hill hornblendes, combined with the slower H diffusion in hornblende, does argue strongly for the meteoric contamination interpretation.

*Fe<sup>2+</sup> and Fe<sup>3+</sup> data*

Results of the wet chemical study of ten augite specimens from this suite show a range of oxidation from 19.3% up to 35.1% of the total Fe as Fe<sup>3+</sup> (Table 4). These values are within the ranges for Fe<sup>3+</sup> proposed by previous Mössbauer studies. Wet chemical data were then used as “true” Fe<sup>3+</sup> contents to provide a check on the interpretation of various models of our Mössbauer data (“M.E.” on Table 4) and, ultimately, as part of the calculation of improved *C* values.

Mössbauer data collected for all 18 samples in our suite were processed to derive several different models for each spectrum, as shown in Table 5. Eight peak fits modeled two (octahedral) Fe<sup>2+</sup> and two (one octahedral and one tetrahedral) Fe<sup>3+</sup> doublets, six peak fits used two Fe<sup>2+</sup> and one Fe<sup>3+</sup>(octahedral) doublet, and four peak fits used one doublet for each oxidation state of Fe (Fig. 1). A comparison of results of these models vs. the wet chemical data is shown in Table 4. These data can be used to illustrate the large differences between fitting models, and to assess the need for correction factors to provide agreement between Mössbauer and wet chemical results. For reasons discussed earlier, a true value of *C* as defined by BANCROFT (1973) cannot be defined for these augites, so we have defined an empirical correction factor (ECF):

$$ECF = \frac{(Fe^{3+}/Fe^{2+}) \text{ by Mössbauer}}{(Fe^{3+}/Fe^{2+}) \text{ by wet chemistry}} \quad (5)$$

Table 3. D/H Data on Dish Hill Samples

	Wt%H <sub>2</sub> O	D/H,‰
Hornblende Ba-5 <sup>1</sup>	1.03	-47.9
Assorted hornblendes <sup>2</sup>	0.93-1.03	-46.8±7.1
Cpx DH-201	0.18	-102.9
Cpx DH-202	0.11	-111.0
Cpx DH-203	0.86	-121.9
Cpx DH-204	0.06	-115.4
Cpx DH-205	0.06	-123.5
Cpx DH-206	0.06	-124.7
Cpx DH-207	0.13	-93.0
Cpx DH-209	0.15	-114.6
Cpx DH-210	0.07	-134.3
Cpx DH-211	0.05	-154.3
Cpx DH-212	0.13	-118.2
Cpx DH-213	0.09	-130.7
Cpx DH-217	0.06	-139.1
Cpx DH-218	0.11	-128.3
Cpx DH-220	0.12	-145.2
Cpx DH-222	0.07	-129.8
Cpx DH-227	0.07	-140.5
Cpx DH-231	0.10	-113.3
Basalt Ba-1-101	0.06	-87.0
Basalt Ba-2-101	2.28	-98.1
Basalt Ba-2-102	1.19	-99.6
Basalt Ba-3-101	1.74	-102.2
Basalt Ba-3-102	1.30	-95.1
Basalt Ba-5-101	0.87	-100.2

<sup>1</sup>Data from DYAR *et al.*, 1992<sup>2</sup>Data from BELL and HOERING, 1994

Table 4. %Fe<sup>3+</sup> Contents and ECF Values from Different Fitting Models as Compared to Wet Chemistry

Sample	Thickness mg Fe /cm <sup>2</sup>	Wet Chemistry %Fe <sup>3+*</sup>	L6_14		L6_11		L6_08**		L8_18**		V4_U	
			%Fe <sup>3+*</sup>	M.E.†	%Fe <sup>3+*</sup>	M.E.						
DH-201	3.74	29.3	29.1	28.9	30.7	34.8	31.0	31.0	30.1	36.6	31.7	
DH-202	3.80	29.6	31.6	24.6	29.3	26.8	27.8	30.2	29.4	30.2	29.7	
DH-203	3.63	30.1	32.5	22.8	28.6	27.3	28.1	32.0	30.9	23.9	27.1	
DH-204	4.30	n.a.	34.0	32.9	31.8	n.f.		32.2	31.1	n.f.		
DH-205	4.06	29.2	31.1	29.5	30.9	29.9	29.2	29.6	28.8	30.1	29.7	
DH-206	4.28	33.3	35.4	34.6	32.1	36.0	31.4	33.8	32.5	45.6	33.9	
DH-207	6.18	n.a.	45.8	43.3	33.8	n.f.		42.9	39.9	n.f.		
DH-209	3.01	19.3	20.5	19.9	27.3	30.3	29.3	19.0	19.2	17.5	23.5	
DH-210	3.01	21.0	28.6	28.9	30.7	21.8	25.3	31.1	30.1	19.1	24.5	
DH-211	4.15	n.a.	35.8	45.3	34.1	n.f.		35.7	33.6	n.f.		
DH-212	4.21	n.a.	30.1	25.6	29.6	n.f.		28.7	28.0	n.f.		
DH-213	3.93	35.1	28.3	53.8	35.2	53.8	35.9	36.3	34.6	19.6	24.8	
DH-217	4.19	n.a.	40.3	34.6	32.1	n.f.		39.3	37.0	n.f.		
DH-218	4.26	n.a.	35.1	47.7	34.4	n.f.		34.2	32.8	n.f.		
DH-220	4.09	n.a.	31.2	27.7	30.3	n.f.		29.9	29.1	n.f.		
DH-222	4.20	31.3	33.0	28.9	30.7	32.9	30.3	31.7	30.7	34.2	31.0	
DH-227	4.34	n.a.	34.0	39.1	33.1	n.f.		32.4	31.3	n.f.		
DH-231	4.45	34.7	38.1	47.2	34.4	45.3	34.0	37.0	35.1	38.0	32.1	

\*Errors on the wet chemical analyses of our samples are at least as good as  $\pm 0.1\%$  of the %Fe<sup>2+</sup> present, or approximately  $\pm 0.07$  of the %Fe for each species.

†"True" %Fe<sup>3+</sup> was not calculated for L6\_14 fits because the regression line fit to the data was not of significant variance. M.E. represents results obtained using the Mössbauer effect.

\*\*Convergent fits for 6 Lorentzian peaks, 8 constraints and 4 Voigt peaks were not obtained.

Figure 2 presents a comparison between ECF and the Mössbauer Fe<sup>3+</sup>/Fe<sup>2+</sup> for the samples on which wet chemistry was performed. Analysis of variance shows that all of the fits except L6\_14 are significant when outliers are omitted. The regression data on these models are given in Table 5. Figure 2 illustrates the major differences between fitting models. Regression lines derived from these figures can be used to convert Mössbauer Fe<sup>3+</sup>/Fe<sup>2+</sup> to agree with wet chemical Fe<sup>3+</sup>/Fe<sup>2+</sup> for augites in the compositional range studied here. Of course,

this makes the assumption that wet chemistry gives the "true" value for Fe<sup>3+</sup>/Fe<sup>2+</sup>; certainly wet chemistry yields Fe<sup>3+</sup>/Fe<sup>2+</sup> ratios with the smallest errors.

For the purposes of this study, our goal was to determine the Fe<sup>3+</sup>/Fe<sup>2+</sup> ratios of all our samples; therefore, we were forced to choose one consistent model for fitting. Unfortunately, the statistical parameters commonly used to evaluate Mössbauer fits were not helpful in this case. Although  $\chi^2$  values for the fits uniformly declined when additional

Table 5. Models Used to Interpret Mössbauer Results and Regression Results

Model	# of Peaks	# of Doublets	Widths* Constrained?	Areas* Constrained?	Line Shape Used	Intercept	Slope	r
L6_14	6	3	yes	yes	Lorentzian			
L6_11	6	3	yes	no	Lorentzian	0.26	1.62	0.99
L6_8	6	3	no	no	Lorentzian	0.43	1.42	0.96
L8_18	8	4	yes	yes	Lorentzian	0.92	0.28	0.69
V4_U	4	2	no	no	Voigt	0.37	1.51	0.89

\*Widths and areas are constrained to vary in pairs. For example, when the width of one Fe<sup>3+</sup> peak increases, the width of its pair will also be increased by a similar amount.

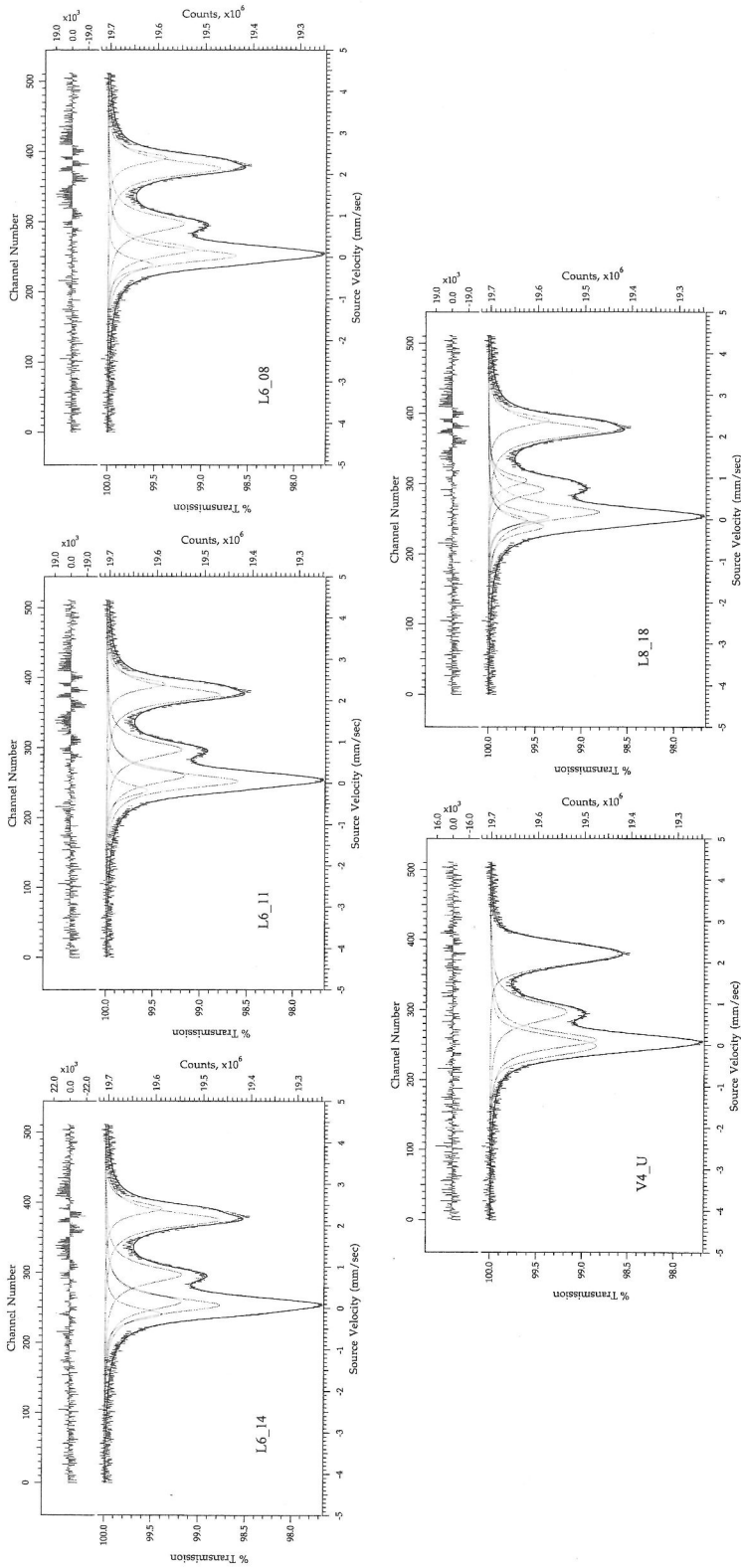


FIG. 1. Mössbauer spectra of augite sample DH-206, fit with the five different models described in Table 5. The total areas of the  $\text{Fe}^{3+}$  doublets in each case are 35.4, 34.6, 36.0, 33.8, and 45.6 for L6\_14, L6\_11, L6\_08, L8\_18, and V4\_U respectively; the total  $\text{Fe}^{3+}$  as determined by wet chemistry is 33.3% of the total iron.

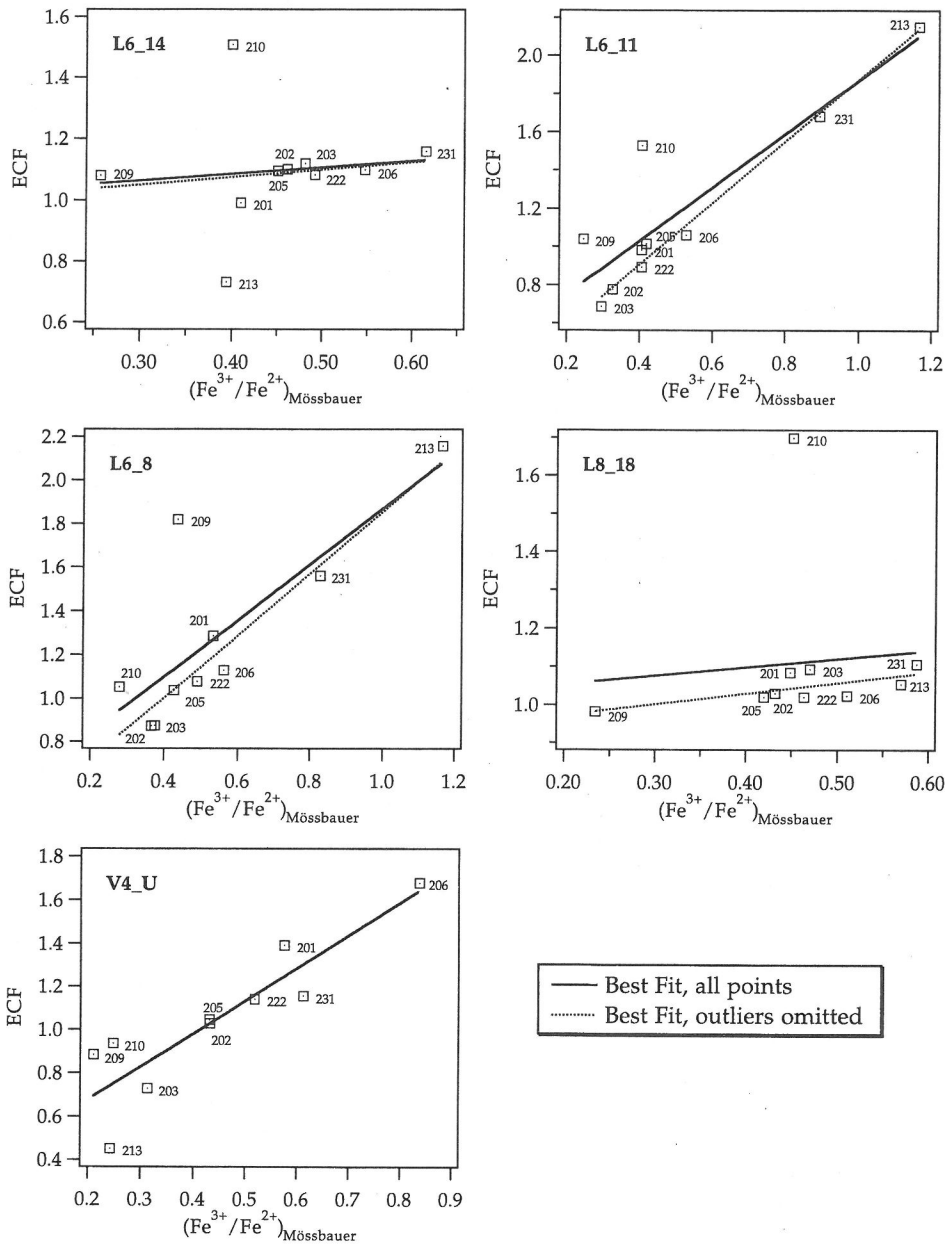


FIG. 2. The relationship between ECF and Mössbauer  $\text{Fe}^{3+}/\text{Fe}^{2+}$  is plotted for each of the five models presented in Table 5, with regression lines shown as before. Analysis of variance shows that all of the dashed line fits except L6\_14 are significant. The equations of these regression lines may be used to calculate 'true'  $\text{Fe}^{3+}/\text{Fe}^{2+}$  from Mössbauer results when the fitting model is known.

doublets were added to the fits (*i.e.*, going from four to six to eight peak fits), the improvement was not dramatic, and may be completely due to improvement in the fit to the spectral noise (as suggested by RUBY, 1973). Either Al or  $\text{Fe}^{3+}$  (or

possibly some combination of the two) might occupy the tetrahedral sites in the structures, so that crystal chemistry does not distinguish between fitting models. No X-ray diffraction data were available to assist in distinguishing the six peak models

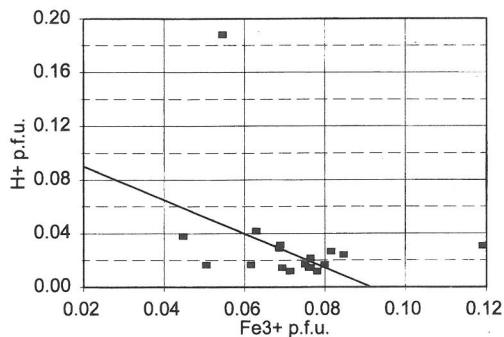


FIG. 3. Plot of  $\text{Fe}^{3+}$  vs.  $\text{H}^+$  contents of samples, with a line of slope =  $-1$ .

from the eight peak models. Accordingly, in this study we have made an arbitrary choice to use the Mössbauer  $\text{Fe}^{3+}/\text{Fe}^{2+}$  results from L6\_11 fits to determine the "true"  $\text{Fe}^{3+}/\text{Fe}^{2+}$  values used to recalculate the formulas given in Table 2. The L6\_11 model was chosen because it yields the best fit ( $r = 0.99$ ) to the wet chemical data.

#### Comparison of $\text{H}^+$ and $\text{Fe}^{3+}$

It might be tempting to use the data collected here to look for dependent relationships between  $\text{H}^+$  and  $\text{Fe}^{3+}$  as predicted by the dehydrogenation mechanism discussed above. However, Fig. 3 demonstrates that it would be risky to do so. Error bars on the  $\text{H}^+$  determinations are extremely large, making any correlation between  $\text{H}^+$  and  $\text{Fe}^{3+}$  extremely tenuous. Unless the unusually high  $\text{H}^+$  content sample is included, points on this plot do not define a real trend. In a qualitative fashion, this plot suggests that an upper limit for a hydrogenated augite in the mantle might be on the order of 0.05 or 0.20  $\text{H}^+$  ions per formula unit (p.f.u.) if all the  $\text{Fe}^{3+}$  in the augite is assumed to be the result of dehydrogenation. Conversely, a maximum amount of  $\text{Fe}^{3+}$  that might occur in a fully dehydrated augite following eruption might be about 0.20  $\text{Fe}^{3+}$  atoms p.f.u. However, these values are questionable due to the lack of precision in the respective analyses.

#### Results of dehydration experiments

After each heat treatment experiment on a diopside crystal, we measured the infrared spectrum of the sample. Figure 4 shows a sequence of infrared spectra taken after a series of heat treatments of a sample of Jaipur diopside at  $810^\circ\text{C}$ , indicating the progressive loss of water

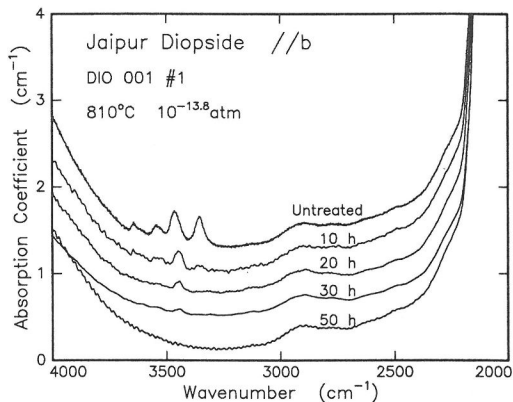


FIG. 4. Sequence of infrared absorption spectra of a sample of Jaipur diopside after treatment for cumulative times of 0, 10, 20, 30 and 50 hours at  $810^\circ\text{C}$ , with the oxygen activity controlled at  $10^{-13.8}$  atm. The absorption bands near  $3500\text{ cm}^{-1}$  correspond to O-H stretching vibrations.

at high temperature. Because our samples were prepared as thin slabs, and assuming isotropic diffusion of hydrogen (INGRIN *et al.*, 1995), we were able to use a theoretical analysis for diffusion in an infinite slab to calculate hydrogen diffusivities as a function of temperature for our samples. Figure 5 shows values of the water con-

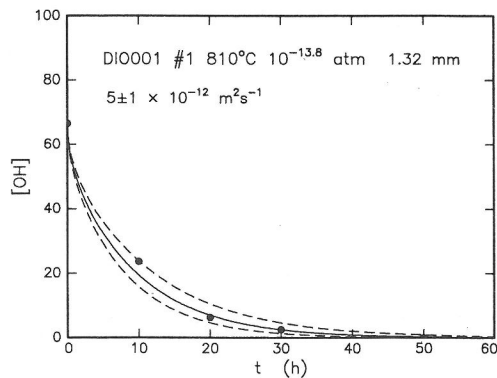


FIG. 5. Dehydration kinetics for the sample of Jaipur diopside illustrated in Fig. 5 showing dehydration after a range of heat treatment times at  $810^\circ\text{C}$ . The concentrations of OH were determined by integrating the area beneath the O-H bands in the spectra shown in Fig. 4. The solid line is a fit to the data using a solution of Fick's law for diffusion in an infinite slab of finite thickness, yielding a diffusivity for hydrogen of  $5 \times 10^{-12}\text{ m}^2\text{ s}^{-1}$ . The dashed lines correspond to  $4$  and  $6 \times 10^{-12}\text{ m}^2\text{ s}^{-1}$ . Note that essentially all the H is diffused out of these samples by 50 hours at this temperature.

tent of the Jaipur diopside sample from Fig. 4 as a function of time. A fit to the data, assuming isotropic diffusion in a slab, is superimposed on the figure and indicates a diffusivity of  $D_{H^+} = (5 \pm 1) \times 10^{-12} \text{ m}^2\text{s}^{-1}$ . We have performed similar analyses on samples treated at  $750^\circ\text{C}$ . Fig. 6 shows a comparison of these results with those of INGRIN *et al.* (1995) for a diopside with  $\sim 50\%$  lower Fe content. Also shown are values for hydrogen diffusion in diopside and augite, calculated from the results of SKOGBY and ROSSMAN (1989) using the infinite slab model for diffusion. We have also plotted in Fig. 6 the hydrogen diffusivities determined in olivine (MACKWELL and KOHLSTEDT, 1990), and hornblende (GRAHAM *et al.*, 1984), and water diffusivities in rhyolite glass (ZHANG *et al.*, 1991). The hornblende curve was determined by a linear regression fit to the data for both hornblende samples reported by

GRAHAM *et al.*, assuming a plate geometry. The clinopyroxene diffusion data from the various studies span a wide range in hydrogen diffusivity at any temperature. Because the only apparent compositional difference between the clinopyroxene is the Fe content, a positive correlation appears to exist between the Fe content and the hydrogen diffusivity (Fig. 6). Thus, we would expect that if we were to include the Dish Hill augites in Fig. 6, they would fall in the upper range of hydrogen diffusivities measured for clinopyroxene.

## DISCUSSION

### *Implications for mantle $f_{O_2}$*

Traditionally, petrologic studies of mantle xenoliths have been used to gain information about mantle lithologies, mineral compositions, P-T conditions, and major and trace element effects of fluid-rock interactions in the mantle. These studies have made the assumption that major, trace, and rare earth element (REE) compositions of mantle xenoliths are not significantly changed during transport to the surface. The relatively fast rate of transport (hours to weeks) compared to the slow rates of diffusion of large major and trace element cations in mantle minerals makes this assumption fairly safe. In contrast, many recent studies measure  $\text{Fe}^{3+}/\text{Fe}^{2+}$ ,  $\text{H}^+$  contents, and D/H ratios in mantle samples and use these data to make inferences about mantle  $f_{O_2}$  conditions and mantle fluid/rock interactions. Such inferences are risky because D and H diffusion rates are generally orders of magnitude faster in mantle minerals than major element diffusion rates, and dehydrogenation may change the  $\text{Fe}^{3+}/\text{Fe}^{2+}$  ratio in the process. It is important to know if measured  $\text{Fe}^{3+}/\text{Fe}^{2+}$ , D/H and  $\text{H}^+$  contents actually represent original mantle values, or if they may have been altered during transport.

### *Dehydrogenation of minerals*

During transport of basalt and included megacrysts from their sources deep in the Earth to the surface, hydrogen and deuterium dissolved in the minerals and melt will partially exchange, and some interactions with meteoric water in the country rock may occur. In particular, minerals containing dissolved water in a subsolidus environment may dehydrate significantly during entrainment and transport in an undersaturated melt phase. The degree of dehydration will depend on the partitioning of water among the various phases, the kinetics of water diffusion within the crystals and

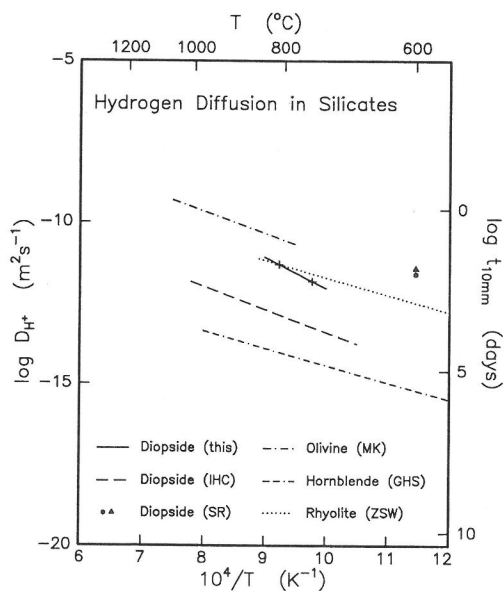
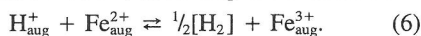


FIG. 6. Hydrogen diffusion in silicates, based on data for hornblende from GRAHAM *et al.* (1984) GHS, for diopside and augite from SKOGBY and ROSSMAN (1989) SR, for olivine from MACKWELL and KOHLSTEDT (1990) MK, for diopside by INGRIN *et al.* (1995) IHC, and for diopside in the present study (this). Also shown are data for water diffusion in rhyolite glass by ZHANG *et al.* (1992) ZSW. Horizontal axes show temperature (top) and inverse temperature (bottom axis); the left vertical axis shows the log of hydrogen diffusivity, while the right vertical axis shows the log of time expressed in days for diffusive loss of 90% of the hydrogen from 10 mm thick slabs. Of the three diopside data sets, the Ingrin data are for the most iron-poor composition, and the Skogby and Rossman data are for the most iron-rich compositions.

melt, and the temperature/time history of entrainment and transport.

Some constraints on water exchange are provided by experimental investigations of the kinetics of hydration and dehydration of the appropriate minerals and melts. DYAR *et al.* (1993) used hydrogen diffusion data in hornblende (GRAHAM *et al.*, 1984) to infer the history of H<sup>+</sup> loss (and a parallel increase in Fe<sup>3+</sup>/Fe<sup>2+</sup>) in a suite of mantle-derived hornblendes, with inferences for mantle metasomatic processes. In this way, they were able to show that significant H<sup>+</sup> loss from hornblende must have occurred due to a metasomatic event in the mantle prior to entrainment. Other studies have investigated the rates of hydration/dehydration of minerals such as olivine (MACKWELL and KOHLSTEDT, 1990), and diopside (SKOGBY and ROSSMAN, 1989; SKOGBY, 1994; INGRIN *et al.*, 1995). There are also indications that equilibration of point defect concentrations in mineral grains will take significantly longer than H<sup>+</sup> transport rates, so that changes in H<sup>+</sup> content will be accompanied by changes in Fe<sup>3+</sup>/Fe<sup>2+</sup>, according to the reaction



For example, at temperatures of about 1200°C, dehydration of olivine with a 10 mm grain size will take only 4 hours, while point defect equilibration (and hence equilibration of Fe<sup>3+</sup>/Fe<sup>2+</sup>) will take about 4 days (MACKWELL *et al.*, 1988; MACKWELL and KOHLSTEDT, 1990).

As discussed above, we have extended the data on H<sup>+</sup> diffusion in diopside compositions (INGRIN *et al.*, 1995) to Fe-rich clinopyroxene compositions (augite). In the absence of diffusion measurements for deuterium in clinopyroxene, we speculate that the kinetics of deuterium diffusion in these minerals are likely to be equal to or slower than that for hydrogen, depending on the nature of the diffusing species (H<sub>2</sub>O/D<sub>2</sub>O or H<sup>+</sup>/D<sup>+</sup>). In addition, although no water diffusion measurements have been reported in molten basalt or basalt glass, a number of studies have investigated water transport for relatively silica-rich magma and glass compositions (KARSTEN *et al.*, 1982; LAPHAM *et al.*, 1984; ZHANG *et al.*, 1991). We use these results and the observations of H<sub>2</sub>O contents, D/H ratios, and Fe<sup>3+</sup>/Fe<sup>2+</sup> ratios in Dish Hill, California basalts and megacrysts to infer the history of H and D exchange during the transport of the magma and included minerals from their sources to the surface at Dish Hill.

#### *Mantle sources and alteration of Dish Hill basalt and megacrysts*

The compositional data compiled from Dish Hill basalts and included megacrysts, coupled with the

diffusion information described above provide insight into the origins of the various rock and mineral compositions and the effects of their entrainment and transport history. Clearly the basalt was generated at depth in the Earth, and it entrained the xenoliths and megacrysts during transport to the Earth's surface. It is noteworthy that a basaltic magma will be initially undersaturated with water, and therefore water dissolved in entrained minerals might be expected to partition strongly into the melt at a rate dependent on either the diffusion of hydrogen in the mineral (KARATO, 1986) or of water through the melt (ZHANG *et al.*, 1991), whichever is slower.

The right hand axis of Fig. 6 provides an indication of the rates of hydrogen loss at any particular temperature from 10 mm grains of natural olivine, hornblende, and clinopyroxene of various Fe contents. Thus, in a dehydrating environment, a grain of forsteritic (mantle composition) olivine 10 mm across will lose 90% of its water in about 4 hours at 1200°C. By contrast, a 10 mm grain of hornblende will take several years for 90% dehydration under the same conditions. The diopside grains used in this study will give dehydration rates similar to olivine under these conditions; grains with higher Fe contents are likely to yield even faster transport rates for hydrogen. Also shown on Fig. 6 is the diffusivity for water in rhyolite compositions determined by ZHANG *et al.* (1991), who demonstrated that the mobile hydrogen-bearing species in rhyolitic glasses and melts is molecular water. Centimeter-scale transport of water in these materials might be expected to occur in about 2 days at 1200°C; however, transport rates in less polymerized glass and melts of higher Fe (and Si-poorer) compositions, such as basalt, may be faster.

The observed partial breakdown of the Dish Hill hornblende megacryst samples provides an indication of the temperatures (probably 1100°–1250°C) during transport, and of the time scales for entrainment and ascent that are likely to take from several days to a month (*e.g.*, SPERA, 1984). While it is not clear that the basalt and megacrysts have a common depth of origin, oxygen isotope studies by FARMER *et al.* (1995) indicate that both are derived from a mantle source. The D/H ratios for the basalts are very uniform and show that some mixing with meteoric water has occurred during transport, presumably due to contact metamorphism of the country rock by the melt and to interactions between the melt and shallow crustal hydrothermal fluids. Although the diffusion rate for water in silicate melts and glasses suggests relatively short diffusion distances over the time required to transport

magma to the surface (Fig. 6), turbulent mixing could provide a more effective mechanism for homogenization of D/H ratios within the magma during ascent. The D/H ratios for the hornblende megacrysts are consistent with a mantle source region and show little evidence of exchange with the surrounding basalt, as might be expected given the relatively slow diffusion rates for hydrogen in hornblende. By contrast, the fine-grained hornblende selvages on composite xenoliths show some exchange with the magma; because 1 mm grains equilibrate approximately 100 times faster than 10 mm grains, this observation does not suggest a different origin for the xenoliths and the megacrysts.

Based on the kinetics of hydrogen diffusion in clinopyroxene, augite megacrysts would be expected to exchange hydrogen with a surrounding basaltic melt on time scales much less than those required for transport to the surface. Thus, rapid hydrogen loss might be anticipated during mobilization, resulting in an increase in the  $\text{Fe}^{3+}/\text{Fe}^{2+}$  in the augite, following eqn. (6). The diffusion of  $\text{D}^+$  in clinopyroxene is expected, on steric grounds, to be slower than the diffusion of  $\text{H}^+$ . Thus, loss of  $\text{D}^+$  from the clinopyroxene may lag behind the loss of  $\text{H}^+$ , resulting in a transient increase in D/H. While there are no data to constrain this supposition, it might provide a reason for the observed higher D/H in the augite than in the basalt. Such an effect would produce augites that were zoned in D/H. Any variation in D/H ratios and in  $\text{Fe}^{3+}/\text{Fe}^{2+}$  may thus result from hydrogen exchange with the basalt during transport, and would not necessarily reflect mantle compositions.

In contrast, diffusion rates are likely to be similar for  $\text{H}_2\text{O}$  and  $\text{D}_2\text{O}$  in the basalt. Due to convective mixing in the magma, no equivalent compositional zoning of D/H or  $\text{Fe}^{3+}/\text{Fe}^{2+}$  is likely to be observed in the basalt. If  $\text{D}^+$  and  $\text{H}^+$  can diffuse so rapidly in large megacrysts (*i.e.*, on the time scales of transport), then dehydrogenation must also occur within the smaller grains in polycrystalline xenoliths, due to greater rates of grain boundary diffusion compared to rates of lattice transport.

## CONCLUSIONS

(1) Mössbauer spectra measured on a suite of 18 mantle aluminous augite samples reveal a range of  $\text{Fe}^{3+}$  doublet areas from 14%  $\text{Fe}^{3+}$  to 60%  $\text{Fe}^{3+}$ . Spectra are interpreted with simple three doublet models constrained by holding peak widths constant in doublet pairs; more complicated fits are also mathematically possible.

(2)  $\text{H}^+$  contents as determined by uranium ex-

traction techniques range from 0.06 to 0.18 wt%  $\text{H}_2\text{O}$  for augite (with an outlier at 0.86 wt%  $\text{H}_2\text{O}$ ), and 0.06 to 2.28 wt%  $\text{H}_2\text{O}$  for their entraining basalts.

(3) Hydrogen isotope data range from  $-93.0\text{‰}$  to  $-154.3\text{‰}$ , for augite, and  $-87.0\text{‰}$  to  $-102.2\text{‰}$  for related basalts. Both basalt and augite samples show evidence of contact and exchange with meteoric waters either during ascent or cooling, and they are distinctly different from hornblendes previously reported from the Dish Hill locality.

(4) Predictions of hydrogen transport based on diffusion data for hydrogen and water in augites and basalt are consistent with observations of significant interactions with meteoric water during transport to the surface of the Earth, while similar data for amphibole indicate that hornblende megacrysts will exchange little on the timescales of transport, as observed by BELL and HOERING (1994).

(5) The lack of a clear systematic trend in  $\text{H}^+$  versus  $\text{Fe}^{3+}$  data could be masked by the uncertainties in the hydrogen analysis; it could also suggest significant variability in  $\text{H}^+$  or  $\text{Fe}^{3+}$  contents of augite in the mantle source region.

*Acknowledgments*—Supported by National Science Foundation grants EAR-9304304 and EAR-9405310 (M.D.D.), EAR-9305187 (S.J.M.), EAR-9005414 and EAR-9315762 (A.V.M.), with travel assistance provided by Navajo Community College. We thank Howard Wilshire and Jane Nielson for their guidance and assistance with sample collection, Sanjay Monie at Penn State for assistance with IR spectroscopy, Joseph W. Stucki and analyst Jun Wu at the University of Illinois for wet chemical data, and Kipp Bajaj, Heather Wilcox, and Marjorie Taylor for assistance with sample preparation and Mössbauer spectral data reduction. Thorough and constructive reviews of this manuscript were generously provided by Jane Nielson, Colin Graham, and Catherine McCammon.

## REFERENCES

- AMTHAUER G., ANNERSTEN H. and HAFNER S. S. (1976) The Mössbauer spectrum of  $^{57}\text{Fe}$  in silicate garnets. *Zeits. Krist.* **143**, 14–55.
- BAI Q. and KOHLSTEDT D. L. (1992) Substantial hydrogen solubility in olivine and implications from water storage in the mantle. *Nature* **357**, 672–674.
- BANCROFT G. M. (1967) Quantitative estimates of site populations in an amphibole by the Mössbauer effect. *Phys. Lett.* **26A**(1), 17–18.
- BANCROFT G. M. (1969) Quantitative site population in silicate minerals by the Mössbauer effect. *Chem. Geol.* **5**, 1969, 255–258.
- BANCROFT G. M. (1973) *Mössbauer Spectroscopy. An Introduction for Inorganic Chemists and Geochemists.* McGraw-Hill.
- BANCROFT G. M. and BURNS R. G. (1967) Interpretation of the electronic structure of iron in pyroxenes. *Amer. Mineral.* **52**, 1278–1282.

- BANCROFT G. M., BURNS R. G. and HOWIE R. A. (1967a) Determination of the cation distribution in the orthopyroxene series by the Mössbauer effect. *Nature* **213**, 1221–1223.
- BANCROFT G. M., BURNS R. G. and MADDOCK A. G. (1967b) Determination of cation distribution in the cummingtonite-grunerite series by Mössbauer spectroscopy. *Amer. Mineral.* **52**, 1009–1026.
- BANCROFT G. M. and BROWN J. R. (1975) A Mössbauer study of coexisting hornblendes and biotites: Quantitative  $\text{Fe}^{3+}/\text{Fe}^{2+}$  ratios. *Amer. Mineral.* **60**, 265–272.
- BELL D. R. (1993) Hydroxyl in mantle minerals. Ph.D. Thesis, California Institute of Technology.
- BELL D. R. and HOERING T. C. (1994) D/H ratios and  $\text{H}_2\text{O}$  contents of mantle-derived amphibole megacrysts from Dish Hill, California. *Lunar Planet. Inst. Conf. on Deep Earth and Planetary Volatiles*.
- BELL D. R. and ROSSMAN G. R. (1992) Water in earth's mantle: The role of nominally anhydrous minerals. *Science* **255**, 1391–1397.
- BIGEISEN J., PERLMAN M. L. and PROSSER H. C. (1952) Conversion of hydrogenic materials to hydrogen for isotopic analysis. *Anal. Chem.* **24**, 1356–1357.
- BRYNDZIA L. T. and WOOD B. J. (1990) Oxygen thermobarometry of abyssal spinel peridotites: The redox state and C-O-H volatile composition of the Earth's sub-oceanic upper mantle. *Amer. J. Sci.* **290**, 1093–1116.
- BURNS R. G. (1966) Origin of optical pleochroism in orthopyroxenes. *Mineral. Mag.* **35**, 715–719.
- CARPENTER S. (1996) The kinetics of hydrogen diffusion in single crystal clinopyroxene. M.S. Thesis, Pennsylvania State University.
- DELOULE, E., ALBARÈDE, F. and SHEPPARD, S. M. F. (1991) Hydrogen isotope heterogeneities in the mantle from ion probe analysis of amphiboles from ultramafic rocks. *Earth Planet. Sci. Letts.* **105**, 543–553.
- DEGRAVE E. and VAN ALBOOM A. (1991) Evaluation of ferrous and ferric Mössbauer fractions. *Phys. Chem. Mins.* **18**, 337–342.
- DYAR M. D. (1984) Precision and interlaboratory reproducibility of measurements of the Mössbauer effect in minerals. *Amer. Mineral.* **69**, 1127–1144.
- DYAR M. D., MCGUIRE A. V. and ZIEGLER R. D. (1989) Redox equilibria and crystal chemistry of coexisting minerals from spinel lherzolite mantle xenoliths. *Amer. Mineral.* **74**, 969–980.
- DYAR M. D., MACKWELL S. M. and MCGUIRE A. V. (1992)  $\text{Fe}^{3+}/\text{H}^+$  and D/H in mantle kaersutites - Missing indicators of mantle fugacities. *Geology* **20**, 565–568.
- DYAR M. D., MACKWELL S. J., MCGUIRE A. V., CROSS L. R. and ROBERTSON J. D. (1993) Crystal chemistry of  $\text{Fe}^{3+}$  and  $\text{H}^+$  in mantle kaersutite: Implications for mantle metasomatism. *Amer. Mineral.* **78**, 968–979.
- EVANS M. J. and BLACK P. J. (1970) Voigt profile of Mössbauer transmission spectra. *J. Phys. C* **3**, 2167–2177.
- FARMER G. L., GLAZNER A. F., WILSHIRE H. G., WOODEN J. L., PICKTHORN W. J. and KATZ M. (1995) Origin of the later Cenozoic basalts at the Cima volcanic field, Mojave Desert, California. *J. Geophys. Res.* **100**, 8399–8415.
- FREY F. A. and PRINZ M. (1978) Ultramafic inclusions from San Carlos, Arizona: Petrologic and geochemical data bearing on their petrogenesis. *Earth Planet. Sci. Lett.* **38**, 129–176.
- GRAHAM C. M., HARMON R. M. and SHEPPARD S. M. F. (1984) Experimental hydrogen isotope studies: Hydrogen isotope exchange between amphibole and water. *Amer. Mineral.* **69**, 128–138.
- GRANT C. A. (1995) Sources of experimental and analytical error in measurements of the Mössbauer effect in amphibole. Ph.D. Thesis, University of Oregon.
- HOLDAWAY M. J., DUTROW B. L., BORTHWICK J., SHORE P., HARMON R. S., and HINTON R. W. (1986) H content of staurolite as determined by H extraction line and ion microprobe. *Amer. Mineral.* **71**, 1135–1141.
- INGRIN J., HERCULE S. and CHARTON T. (1995) Diffusion of hydrogen in diopside: Results of dehydration experiments. *J. Geophys. Res.* **100**, 15489–15499.
- INTERNATIONAL ATOMIC ENERGY AGENCY (1979) Environmental isotope data No. 6, World survey of isotope concentration in precipitation (1972–1975). I.A.E.A. Techn. Rep. Ser. **192**, I.A.E.A. Vienna.
- KARATO S. (1986) Does partial melting reduce the creep strength of the upper mantle? *Nature* **319**, 309–310.
- KARFUNKEL U. and POLLAK H. (1993) A new approach to the determination of the  $\text{Fe}(3+)/\text{Fe}(2+)$  ratio and recoil-free factors in two garnets by Mössbauer spectroscopy. *Phys. Stat. Solidi* **180B**, 6772.
- KARSTEN J. L., HOLLOWAY J. R. and DELANEY J. R. (1982) Ion microprobe studies of water in silicate melts: Temperature-dependent water diffusion in obsidian. *Earth Planet. Sci. Lett.* **59**, 420–428.
- KOMANDEL P. and STUCKI J. W. (1988) The quantitative assay of minerals for  $\text{Fe}^{2+}$  and  $\text{Fe}^{3+}$  using 1,10-phenanthroline: III. A rapid photochemical method. *Clays Clay Mins.* **36**, 379–381.
- LAPHAM K. E., HOLLOWAY J. R., HERVIG R. L. and STOLPER E. M. (1984) Diffusion of  $\text{H}_2\text{O}$  and  $\text{D}_2\text{O}$  in obsidian at elevated temperatures and pressures. *J. Non-Cryst. Solids* **67**, 179–191.
- LONG G. (1963) Interpretation of experimental Mössbauer spectrum areas. *Nucl. Instr. Methods* **24**, 425–428.
- LONG G. J., CRANSHAW T. E. and LONGWORTH G. (1984) The ideal Mössbauer absorber thickness. *Mössbauer Effect Ref. Data J.* **6**(2), 42–49.
- LUTH R. W., VIRGO D., BOYD F. R. and WOOD B. J. (1990) Ferric iron in mantle-derived garnets. *Contrib. Mineral. Petrol.* **104**, 56–72.
- LUTH R. W. and CANIL D. (1993) Ferric iron in mantle-derived pyroxenes and a new oxybarometer for the mantle. *Contrib. Mineral. Petrol.* **113**, 236–248.
- MACKWELL S. J., DIMOS D. and KOHLSTEDT D. L. (1988) Transient creep of olivine: Point defect relaxation times. *Philos. Mag.* **57**, 779–789.
- MACKWELL S. J. and KOHLSTEDT D. L. (1990) Diffusion of hydrogen in olivine: Implications for water in the mantle. *J. Geophys. Res.* **95**, 5079–5088.
- MCGUIRE A. V., DYAR M. D. and WARD K. W. (1989) Neglected  $\text{Fe}^{3+}/\text{Fe}^{2+}$  ratios—a study of  $\text{Fe}^{3+}$  content of megacrysts from alkali basalts. *Geology* **17**, 687–690.
- MCGUIRE A. V., DYAR M. D. and NIELSON J. E. (1991) Metasomatic oxidation of upper mantle peridotite. *Contrib. Mineral. Petrol.* **107**, 252–264.
- MILLER G. H., ROSSMAN G. R. and HARLOW G. E. (1987) The natural occurrence of hydroxide in olivine. *Phys. Chem. Minerals* **14**, 461–472.
- PATERSON M. S. (1982) The determination of hydroxyl by infrared absorption in quartz, silicate glasses and similar materials. *Bull. Mineral.* **105**, 20–29.
- PRESTON R. S., HANNA S. S. and HEBERLE J. (1962) Mössbauer effect in metallic iron. *Phys. Rev.* **128**, 2207–2218.

- RUBY S. L. (1973) Why Misfit when you already have  $\chi^2$ ? In I.J. Gruverman, C.W. Seidel, and D.K. Dieterly, eds., *Mössbauer Effect Methodology* **9**, 277–305.
- SKOGBY H. (1994) OH incorporation in synthetic clinopyroxene. *Amer. Mineral.* **79**, 240–249.
- SKOGBY H. and ROSSMAN G. R. (1989) OH<sup>-</sup> in pyroxene: An experimental study of incorporation mechanisms and stability. *Amer. Mineral.* **74**, 1059–1069.
- SKOGBY H., BELL D. R. and ROSSMAN G. R. (1990) Hydroxide in pyroxene: Variations in the natural environment. *Amer. Mineral.* **75**, 769–774.
- SKOGBY H., ANNERSTEN H., DOMENEGHETTI M. C., MOLIN G. M. and TAZZOLI V. (1992) Iron distribution in orthopyroxene: A comparison of Mössbauer spectroscopy and X-ray refinement results. *Eur. J. Mineral.* **4**, 441–452.
- SMYTH J. R., BELL D. R. and ROSSMAN G. R. (1991) Incorporation of hydroxyl in upper-mantle clinopyroxenes. *Nature* **351**, 732–735.
- SPERA F. J. (1984) Carbon dioxide in petrogenesis III: Role of volatiles in the ascent of alkaline magmas with special reference to xenolith-bearing mafic lavas. *Contrib. Mineral. Petrol.* **88**, 217–232.
- STUCKI J. W. (1981) The quantitative assay of minerals for Fe<sup>2+</sup> and Fe<sup>3+</sup> using 1,10-phenanthroline: II. A photochemical method. *Soil Sci. Soc. Amer. J.* **45**, 638–641.
- STUCKI J. W. and ANDERSON W. L. (1981) The quantitative assay of minerals for Fe<sup>2+</sup> and Fe<sup>3+</sup> using 1,10-phenanthroline: I. Sources of variability. *Soil Sci. Soc. Amer. J.* **45**, 633–637.
- WHIPPLE E. R. (1972) Quantitative Mössbauer spectra and chemistry of iron. Ph.D. Thesis, Massachusetts Institute of Technology.
- WILSHIRE H. W. and TRASK N. J. (1971) Structural and textural relationships of amphibole and phlogopite in peridotite inclusions, Dish Hill, California. *Amer. Mineral.* **56**, 240–255.
- WILSHIRE H. W. and NIELSON-PIKE J. E. (1986) Upper-mantle xenoliths in alkaline basalt, Dish Hill, California. *Guidebook to S. Calif. Field Trips, G.S.A. Cordilleran Section, 82nd Ann. Mtg.*, Los Angeles, CA, 9–11.
- WILSHIRE H. W., MEYER C. E., NAKATA J. K., CALK L. C., SHERVAIS J. W., NILES J. E. and SCHWARZMAN E. C. (1988) Mafic and ultramafic xenoliths from volcanic rocks of the western United States. *U.S. Geol. Survey Prof. Paper* 1443.
- WOOD B. J. and VIRGO D. (1989) Upper mantle oxidation state: Ferric iron contents of Iherzolite spinels by <sup>57</sup>Fe Mössbauer spectroscopy and resultant oxygen fugacities. *Geochim. Cosmochim. Acta* **53**, 1277–1291.
- ZHANG Y., STOLPER E. M. and WASSERBURG G. J. (1991) Diffusion of water in rhyolitic glasses. *Geochim. Cosmochim. Acta* **55**, 441–456.